Prediction of a research vessel manoeuvring using numerical PMM and free running tests

Kunal Tiwari[*1], K. Hariharan[2a], T.V. Rameesha[1b] and P. Krishnankutty[2c]

[1]*Department of Ocean Engineering, Indian Institute of Technology Madras, Chennai, India*
[2]*Department of Mechanical Engineering, Pusan National University, South Korea-46241*

Abstract. International Maritime Organisation (IMO) regulations insist on reduced emission of CO_2, noxious and other environmentally dangerous gases from ship, which are usually let out while burning fossil fuel for running its propulsive machinery. Contrallability of ship during sailing has a direct implication on its course keeping and changing ability, and tries to have an optimised routing. Bad coursekeeping ability of a ship may lead to frequent use of rudder and resulting changes in the ship's drift angle. Consequently, it increases vessels resistance and also may lead to longer path for its journey due to zigzag movements. These adverse effects on the ship journey obviously lead to the increase in fuel consumption and higher emission. Hence, IMO has made it mandatory to evaluate the manoeuvring qualities of a ship at the designed stage itself. In this paper a numerical horizontal planar motion mechanism is simulated in CFD environment and from the force history, the hydrodynamic derivatives appearing in the manoeuvring equation of motion of a ship are estimated. These derivatives along with propeller thrust and rudder effects are used to simulate different standard manoeuvres of the vessel and check its parameters against the IMO requirements. The present study also simulates these manoeuvres by using numerical free running model for the same ship. The results obtained from both these studies are presented and discussed here.

Keywords: planar motion mechanism; oceanographic research vessel; turning circle manoeuvre; hydrodynamic derivatives

1. Introduction

International Maritime Organisation (IMO) has standards for manoeuvrability of sea going vessels. It is difficult to change manoeuvring characteristics of ship once it has been built. Also, a ship with poor manoeuvring characteristics will cause higher fuel consumption and consequent emission. To cope up with these criteria and requirements, manoeuvring qualities of a ship are advised to be checked even at early design stages. With experimental captive and free running model tests, a designer would be able to predict manoeuvring characteristics of vessel with accuracy, but this is not always feasible for different design options due to the higher cost, time and lack of

∗Corresponding author, Ph.D. Student, E-mail: kt@fourier.in
[a] Ph.D. Student., E-mail: hariharan@pusan.ac.kr
[b] Ph.D., E-mail: tv.ramisha7@gmail.com
[c] Professor, E-mail: pkrishnankutty@iitm.ac.in

availability of experimental facilities. As a solution to this predicament, use of computational fluid dynamics (CFD) is gaining popularity to study and predict manoeuvring qualities of ship.

The vessel taken for present study is an Oceanographic Research Vessels (ORV), which is used to collect ocean data and analyse them to understand the physical, chemical and biological characteristics of seawater, the atmosphere and ocean related factors affecting climate changes. These vessels carry equipment for collecting water samples from a range of depths, including the deep seas, as well as deploy equipment for the hydro-graphic sounding of the seabed, along with numerous other environmental sensors. They also carry divers and unmanned underwater vehicles for local survey and other operations.

In order to understand the manoeuvring quality of ship, an appropriate mathematical model representing its equation of motion is required. For a ship, a nonlinear mathematical model to represent its manoeuvring was first developed by Abkowitz (1964) where he used Taylor series expansion to describe the forces acting on the ship hull. Empirical relations provided by researchers such as Hirano *et al*. (1981) and Kijima and Nakiri (1990) give a rough estimate of the hydrodynamic derivatives, but fails to predict nonlinear and coupled derivatives accurately (Liu *et al*. 2015). More reliable values can be obtained by conducting prescribed captive model tests with ship models, of which Planar Motion Mechanism (PMM) is a widely used method. PMM pioneered by Alex and Morton (1962) is nowadays used extensively for captive model tests to derive hydrodynamic derivatives appearing in ship manoeuvring equations of motion. An estimation of hydrodynamic derivatives for a mariner vessel was done by Strom-Tejsen (1966) using PMM. A different approach using system identification to estimate hydrodynamic derivatives was perused by Karllstrom and Astrom (1981). During the same time, Son and Nomoto (1981) came up with manoeuvring model for *S175* container ship. They predicted the manoeuvring characteristics of this ship by solving the mathematical model containing hull derivatives which were estimated from PMM tests and validated the same with free running model experiments. A few more studies of hydrodynamic derivatives estimated by experimental PMM for various vessel model are given in (Hooft *et al*. 1994, Lee and Shin 1998). An initial CFD method to numerically calculate the force history in PMM motion was carried out by Ohmori (1998) and Nonaka *et al*. (2000). Estimation of hydrodynamic derivatives for an offshore supply vessel and its subsequent use in dynamic positioning is presented by Skjetne *et al*. (2004a). A more detailed estimation of derivatives using CFD for *S175 container ship* is presented in (Janardhanan 2010) for shallow water, for roll effects (Shenoi *et al*. 2016) and in waves (Rameesha and Krishnankutty 2018). Cura-Hochbaum (2011) performed CFD PMM for *very large crude carrier (KVLCC1)* with propeller rotating and rudder at zero deflection. Turning circle and zig-zag (20/20) manoeuvres were simulated with the hydrodynamic derivatives estimated from the numerical PMM. Performance of three different virtual disk propeller models for a ship model turning manoeuvre was studied and presented in (Broglia *et al*. 2013). The different models considered are classical Hough and Ordway model, blade element theory model (BEMT) and Ribners Model ($\alpha = 1\ 3$ in Hough and Ordway model). A 6DOF CFD turning circle and 20/20 zig-zag manoeuvre were conducted for *MARIN 7967* (A surface combatant ship) using Unsteady Reynolds Averaged Navier Stokes (URANS) code *CFDShip-Iowa* in (Carrica *et al*. 2013, Duman and Bal 2017). A body force propeller method for virtual disk was used to simulate the force acting from the propeller. A 2D strip theory based program *ShipX* was used for determining the linear hydrodynamic derivatives for KVLCC2 and these values were used to simulate the turning circle and zig-zag manoeuvre at different water depths in (Kvale 2014). The results were compared with SIMMAN (Stern *et al*. 2011) benchmark data. Force history of a 4.3 m model in pure yaw mode of PMM was calculated for different water depths using URANS solver *naoe-FOAM-SJTU* based on

the open source package *OpenFOAM* in (Liu *et al.* 2015). Shen *et al.* (2014) performed 20/20 zigzag and pull out manoeuvre were performed for KCS, KVLCC2 and DTMB 5415M. The same group (Shen *et al.* 2015) also simulated a 10/10 zigzag manoeuvre for KCS with *openFOAM* software using over-set grid method. An extension to this can be found in (Mofidi and Carrica 2014), where 20/20 Zigzag simulation of KCS model using *CFDship-Iowa* software. Zigzag manoeuvre for KCS in shallow water was numerically simulated and reported that CFD under predicts the yaw and yaw rate by 15% and 20% respectively (Carrica *et al.* 2016). It can be inferred that the turbulence model used may not be appropriate for the flow in question, since at model scale the Reynolds number is relatively small and transition from laminar to turbulent boundary layer will occur at some point along the hull and propeller blades. Latest extension to these studies including a comprehensive numerical study of KCS, incorporating resistance test, self-propulsion test and 10/10 zigzag manoeuvre and simulation of turning circle for a container ship *(DTC)* in waves, are reported in (Mofidi *et al.* 2018) and (Cura-Hochbaum and Uharek 2016). Case study of manoeuvrability in adverse conditions is given in (Shigunov *et al.* 2019). The studies have shown the success of RANSE solvers in appropriate prediction of surface ship manoeuvring qualities at an advance stage of ship design. These studies help in understanding the ship controllability problem at the design stage itself and enable the designer to make necessary alterations in the vessel design so as to recheck and verify the acceptability of the design. Many studies, both numerical and experimental, have been confined to some of the international benchmark ship examples. Of course, these studies highlight the reliability of CFD techniques in ship manoeuvring predictions. Unlike the benchmark ships used by various researchers in literature, the oceanographic research vessel (ORV) considered in present study is a relatively small one and its controllability requirements are more. Moreover, the vessel is also fitted with a retractable bow thruster for safe navigation and position maintenance using dynamic positioning (DP) systems. In the present study, the ORV model is subjected to different modes of PMM oscillations and the hydrodynamic derivatives appearing in the speed and steering equations in surface manoeuvring are determined from different force/moment time history, where one steadied cycle is taken for the analysis. These derivatives along with other coefficient in the equations of motion, terms on the right hand side of equation showing the propeller and rudder effect position them to solve and generate trajectories, as required. The vessel trajectories so created can be used to check the ORV manoeuvring quality. These trajectories are also verified using numerical free running model tests.

2. Mathematical model

Right handed coordinate system is used to define the mathematical equations (refer Fig. 1). The positions (x and y) and orientation (ψ) are described with respect to earth fixed coordinate system ($O_E X_E Y_E Z_E$). The origin of earth fixed coordinate system is taken as the starting point of simulation. The velocities (u, v and r) are described with respect to body fixed coordinate system ($o_b x_b y_b z_b$). The origin of body fixed coordinate system is the intersection point of load waterplane, longitudinal central plane and the midship transverse plane.

The equations of motion for vessel can be described as

$$\mathbf{M\dot{v}} + (\mathbf{C} + \mathbf{D})\mathbf{v} = \boldsymbol{\tau} \tag{1}$$

The system inertia and added mass matrix M is defined as
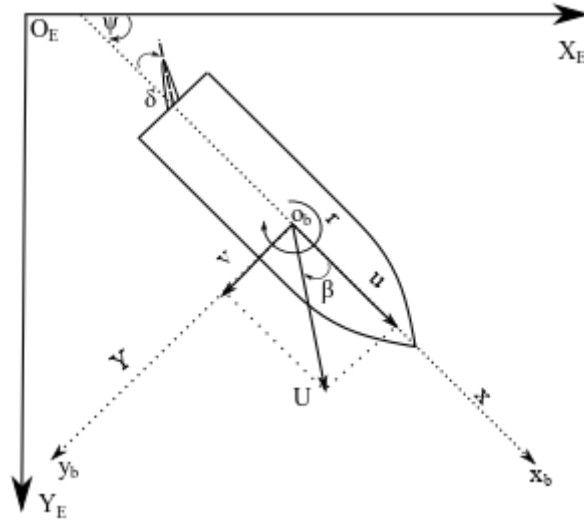
Fig. 1 Earth and Ship Fixed Coordinate systems

$$\mathbf{M} = \begin{bmatrix} m - X_{\dot{u}} & 0 & 0 \\ 0 & m - Y_{\dot{v}} & mx_g - Y_{\dot{r}} \\ 0 & mx_g - N\dot{v} & I_z - N_{\dot{r}} \end{bmatrix} \qquad (2)$$

Damping matrix $\mathbf{D}$ is nonlinear in nature and contains higher order derivatives. It is described as

$$\mathbf{D} = \begin{bmatrix} X_{u|u|}\,|u| & X_{vr}r + X_{vv}v & X_{rr}r \\ 0 & Y_v + Y_{vvv}v^2 + Y_{vrr}r^2 & Y_r + Y_{rrr}r^2 + Y_{vvr}v^2 \\ 0 & N_v + N_{vvv}v^2 + N_{vrr}r^2 & N_r + N_{rrr}r^2 + N_{vvr}v^2 \end{bmatrix} \qquad (3)$$

The Coriolis and centripetal matrix $\mathbf{C}$ is written as

$$\mathbf{C} = \begin{bmatrix} 0 & 0 & Y_{\dot{v}}v \\ 0 & 0 & X_{\dot{u}}u \\ 0 & 0 & 0 \end{bmatrix} \qquad (4)$$

The position and orientation vector $\mathbf{v}$ is defined as

$$\mathbf{v} = \begin{bmatrix} u & v & r \end{bmatrix} \qquad (5)$$

The propeller and rudder force matrix $\boldsymbol{\tau}$ is represented as

$$\boldsymbol{\tau} = \begin{bmatrix} X_P + X_\delta \\ Y_P + Y_\delta \\ N_P + N_\delta \end{bmatrix} \qquad (6)$$

Table 1 Oceanographic research vessel particulars and parameters

Parameter	Prototype	Model (Scale =17.1)
LOA	43.0 m	2.53 m
LBP	39.0 m	2.29 m
B	9.6 m	0.565 m
D	3.7 m	0.218 m
T	2.5 m	0.147 m
LCG	18.11 m	1.065 m
VCG	3.94 m	0.232 m
Displacement	615.95 tonnes	125.37 kg
V	12 knots	1.5 m/s

The mathematical model presented here is a compact version of Son and Nomoto model Son and Nomoto (1981). The only difference is inclusion of $Y_{\dot{r}}$ in the model to have consistency with the Fourier formulation described in (Shenoi 2016). Equation 7-10 are used to calculate the rudder and propeller forces (Son and Nomoto 1981, Dash *et al.* 2015).

$$X_\delta = -F'_N \sin(\delta) \tag{7}$$

$$Y_\delta = -(1+a_H)F'_N \cos(\delta) \tag{8}$$

$$N_\delta = -(1+a_H)x_R F'_N \cos(\delta) \tag{9}$$

$$X_P = (1-t_p)\tau_P \tag{10}$$

The parameter of oceanographic research vessel used in this study are given in Table 1. The model scale is chosen to suit experimental test facility at IIT Madras where the towing tank in department is 85 m long, 3.2 m wide and 3 m deep.

3. HPMM Modes of motion

Horizontal Planar Motion Mechanism (HPMM) is used in towing tanks to perform model tests in three different prescribed oscillation modes, such as pure sway, pure yaw and combined sway-yaw modes, to determine the hydrodynamic derivatives appearing in the equations of motion of surface ship manoeuvring. These derivatives are obtained from steadied one cycle of the time history of surge and sway forces and yaw moment by Fourier series representation and further analysis (refer Appendix).
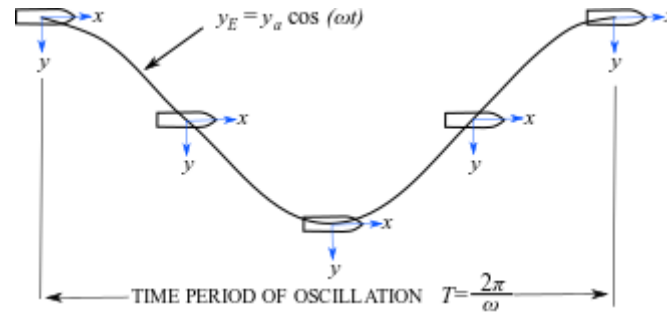
Fig. 2 Path and orientation of model in pure sway mode

3.1 HPMM pure sway mode

In pure sway mode of operation, the model is oscillated sinusoidally in the lateral direction with its axis always parallel to the axis of the towing tank while it is moving forward with a specified speed (Fig. 2). The pure sway mode motion is achieved by oscillating the model described by following equation

$$y_E = y_a \cos(\omega t) \tag{11}$$

$$\psi_E = 0 \tag{12}$$

3.2 HPMM pure yaw mode

In pure yaw mode of operation, the model is oscillated sinusoidally in the lateral direction with its axis always tangential to the sinusoidal path while it is moving forward with a specified speed (refer Fig. 3). The idea is to ensure sway velocity and acceleration is zero. The pure yaw mode motion is obtained by oscillating model described by following equations

$$y_E = y_a \cos(\omega t) \tag{13}$$

$$\psi_E = -\psi_a \sin(\omega t) \tag{14}$$

3.2 HPMM mixed mode

In the combined sway and yaw mode of operation, the model is oscillated sinusoidally in the lateral direction with its axis always having a prescribed drift angle along the sinusoidal path while it is moving forward with a specified speed (refer Fig. 4). This mode is also called as yaw with drift and can be generated with following equations

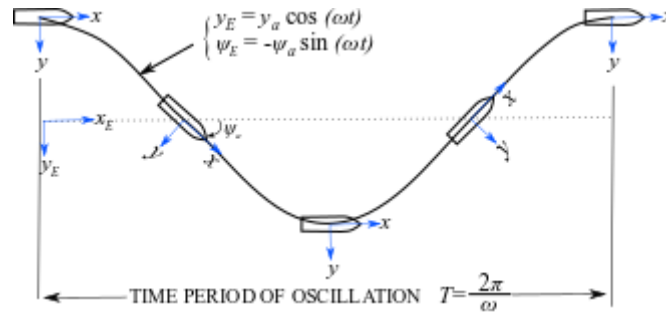$$y_E = y_a \cos(\omega t) \tag{15}$$

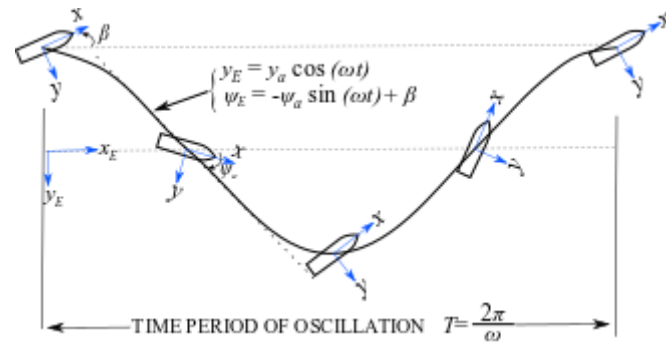Fig. 3 Path and orientation of model in pure yaw mode

Fig. 4 Path and orientation of model in combined sway and yaw mode

Table 2 RMS values of one steady cycle of pure yaw motion for different cell count

| cell count	X (N)	Y (N)	N (Nm)
0.77 M	19.49	5.78	18.32
1.15 M	19.37	6.36	18.42
1.85 M	19.31	6.45	18.45
3.27 M	19.25	6.5	18.46

$$\psi_E = -\psi_a \sin(\omega t) + \beta \tag{16}$$

4. Numerical PMM study

For the present study, dynamic PMM tests are simulated using the planar motion mechanism module available in commercial CFD solver, Star CCM+. The setting in module allow us to simulate a trajectory in x-y plane of laboratory coordinate system while the vessel is free to heave and pitch.
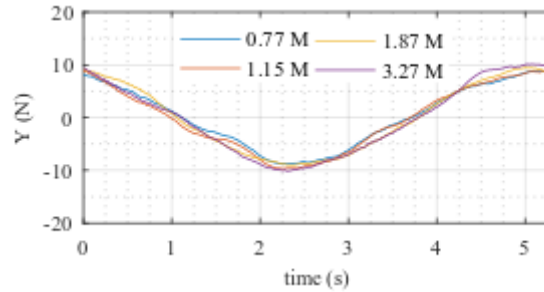
(a) Sway force
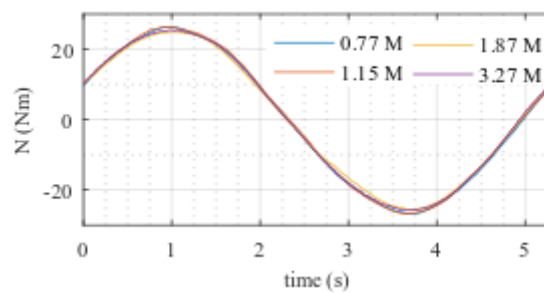
(b) Yaw moment

Fig. 5 Time history of one steady cycle during pure yaw motion for grid independence study

Fig. 6 Boundary conditions

The forward motion is simulated using a flow into the model.

4.1 CFD domain and grid dependancy

According to the International Towing Tank Conference (ITTC) guidelines, suitable computational domain for dynamic tests are chosen by creating a rectangular block around the ship model. Domain dimensions are shown in Fig. 8, which extends 2L from the bow, 4L from stern and 3L from each of port and starboard sides, 1L from deck to top boundary and 1L from keel to bottom sides. An unstructured trimmed hexahedral shape cell with prismatic near wall layers are selected to capture the flow properties. Near wall y+ are kept between 3 and 50 to capture the deformation of the near wall element. Local mesh refinement with high resolution are provided for free surface. Computational mesh generated for the domain and hull is shown in Fig. 7. Grid independent studies

(a)   General

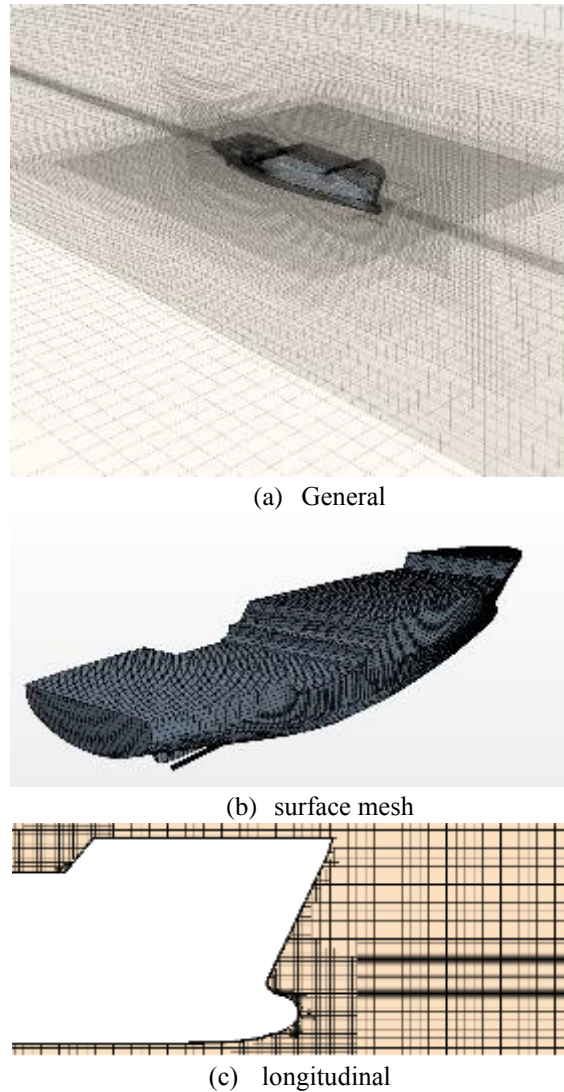
(b)   surface mesh

(c)   longitudinal

Fig. 7 Computational mesh used for PMM simulations

are carried out for proper selection of grid size. Grid refinement ratio of $\sqrt{2}$ for the base cell size is used. Pure yaw tests are carried out for 4 different grid sizes and estimated force and moment time series are plotted in Fig. 5. The RMS value for one steady cycle of force and moment time history is given in Table 2. Based on the convergence of results, grid with cell count of 1.15 M was used to obtain results in other two modes of PMM motion.

4.2 Boundary condition and solver settings

Boundaries of a domain are composed of velocity prescribed at inlet boundary, downstream

pressure at outlet boundary, wall with no slip for the vessel and appendages boundaries and slip wall boundary condition for all other boundaries (Fig. 6). The simulations are unsteady and three dimensional in nature. Transient finite volume simulations employed an implicit unsteady with a segregated (predictor- corrector) flow solver and SIMPLE (Semi Implicit Method for Pressure Linked Equations) solution algorithm. The discretization schemes are kept second order for accurate calculations. Two equation model, realisable model along with two layer all wall y+ treatment is incorporated for turbulence modelling. Free surface modelling is done using VOF method, which captures the movement of the interface between the fluid phases. The High-Resolution Interface Capturing (HRIC) convective discretization scheme is used to track the air-water interface. Based on the value of Courant number at the free surface, a time step value of 0.01s is chosen for the present simulations. All simulations in the present study are run in a super computing facility namely VIRGO super cluster provided by Indian Institute of Technology (IIT), Madras.

4.3 Hydrodynamic forces and derivative determination

Total simulation time for the dynamic simulation varies from 30s to 150s. First and second cycle of the force/moment time history showed fluctuations due to unsteady nature of the flow. After the second cycle steady trends are noticed with the absence of transients, and hence the time series after the second cycle is chosen for the Fourier series analysis. Forces/ moment history obtained from PMM simulations of three different modes are shown in Figs. 9 - 11. Hydrodynamic derivatives are derived from the estimated force-time series using Fourier- series expansion method in which the resulting force/moment is reconstructed as a third order Fourier series. Curve fitting toolbox in MATLAB is used to estimate Fourier coefficients. These Fourier coefficients are compared with the coefficients of the mathematical model for deriving the expression for hydrodynamic derivatives. Estimated hydrodynamic derivatives are included in the Table 3 in non-dimentional form.
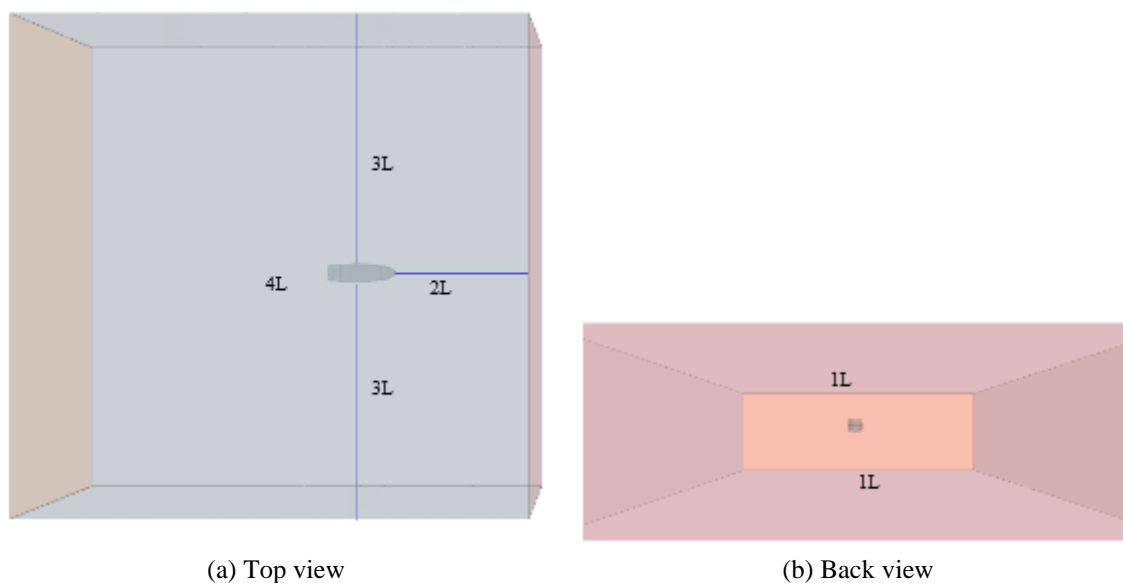

(a) Top view   (b) Back view

Fig. 8 Computational domain used for PMM simulations
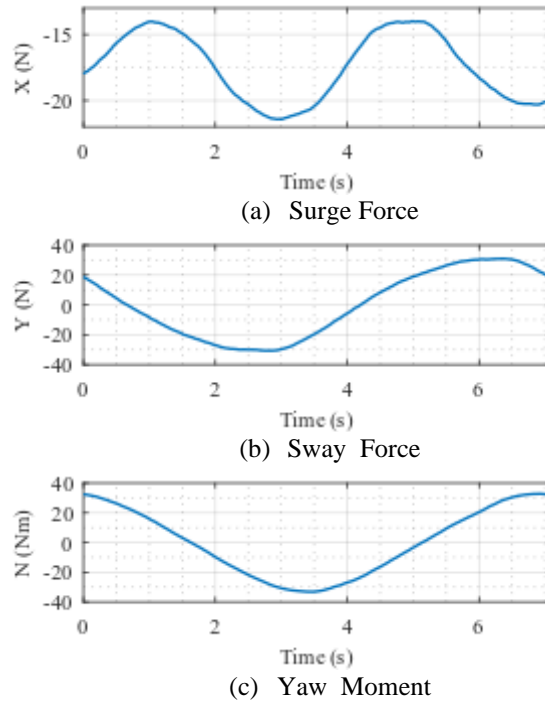
(a) Surge Force

(b) Sway Force

(c) Yaw Moment

Fig. 9 Time history of one steady cycle during pure sway motion

(a) Surge Force

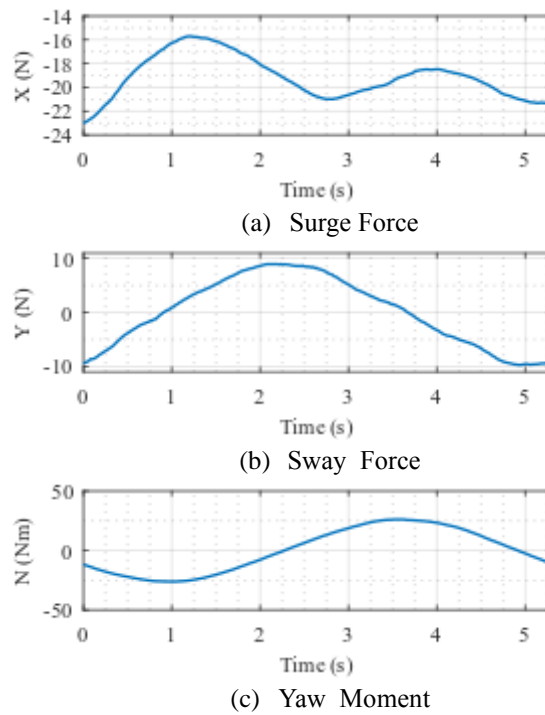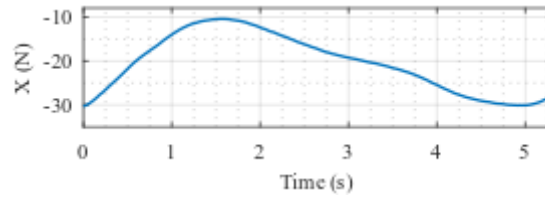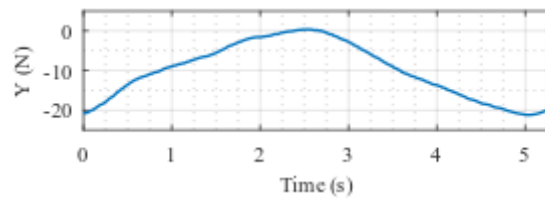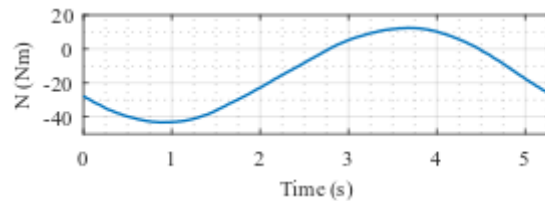(b) Sway Force

(c) Yaw Moment

Fig. 10 Time history of one steady cycle during pure yaw motion
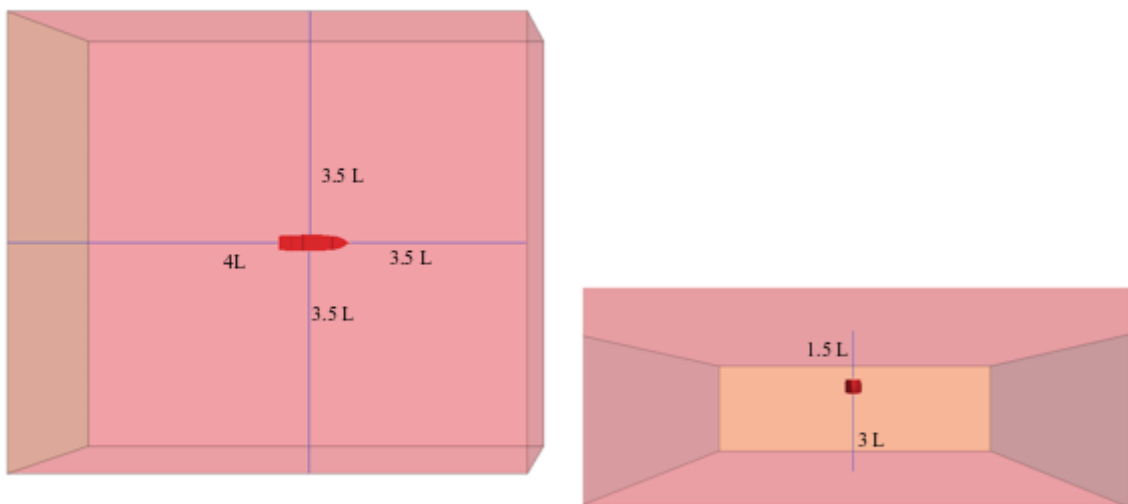
(a) Surge Force

(b) Sway Force

(c) Yaw Moment

Fig. 11 Time history of one steady cycle during mixed mode motion

(a) Top view   (b) Back view

Fig. 12 Computational domain used for free running simulations

Table 3 Hydrodynamic derivatives

Hydrodynamic Derivatives	Value
$X'_{u|u|}$	0.000342112
X'_{vv}	-0.00132208
Y'_{v}	-0.01020213
Y'_{vvv}	-0.01056093
$Y'_{\dot{v}}$	-0.04516673
N'_{v}	-0.00267317
N'_{vvv}	-0.00519088
$N'_{\dot{v}}$	-0.00387776
$X'_{\dot{u}}$	0.00043887
X'_{rr}	-0.00053296
Y'_{r}	-0.00068651
Y'_{rrr}	0.00318686
$Y'_{\dot{r}}$	0.008324624
N'_{r}	0.000556407
N'_{rrr}	0.002129087
$N'_{\dot{r}}$	-0.00151562
X'_{vr}	-0.01054179
Y'_{vrr}	0.060385101
Y'_{vvr}	0.005877106

5. Numerical free running model test

Free running model tests are conducted to predict the manoeuvring characteristics of a vessel in a more direct way compared to other prediction methods. The test involves a scaled down model fitted with rudders and propellers. The rudders and propellers are usually operated using battery powered electric motors.

For the present study, free running model test is numerically simulated using CFD software Star CCM+. Unstructured trimmed hexahedral shape based core mesh is generated using CFD tool. For accuracy near wall region is captured using a prism layer mesh, allowing high-aspect-ratio cells, to provide better resolution for capturing boundary layer. Separate volume mesh provided for free surface, rudder and propeller sections to capture the flow with high resolution. Fig. 13 shows the computational mesh incorporated for free running simulation. Computational domain is created based on the recommended practice by ITTC (Balagopalan *et al.* 2019). Fig. 12 show the
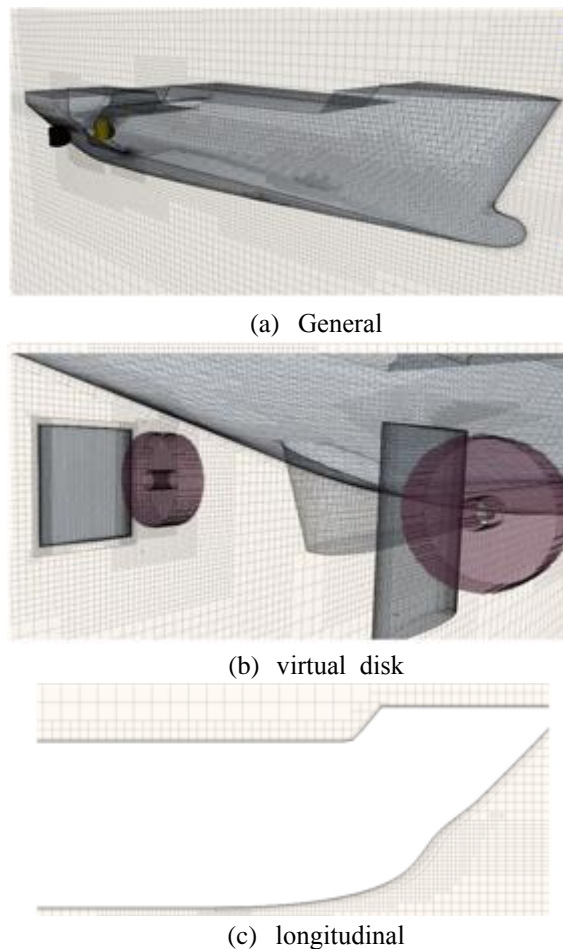

(a) General

(b) virtual disk

(c) longitudinal

Fig. 13 Computational mesh used for free running simulations

computational domain chosen for free running simulation, which extends 3.5L form the bow, 4L from stern and 3.5L from each of port and starboard sides, 1.5L from deck to top boundary and 3L from keel to bottom sides. Domain is selected large enough to avoid wall reflections at outer and side boundary and shallow water effects at bottom boundary. The type of domain boundaries and solver parameters chosen for the direct manoeuvring simulations are same as that of PMM simulations already described in the article. Six degrees of freedom body motion of the free running model is assigned using Dynamic Fluid Body Interaction (DFBI) module available in the StarCCM+. DFBI model enables the solver to obtain fluid induced six degree of freedom motion of the body by solving equations of dynamic motion. Pressure and velocities over the surface of the body is integrated to estimate the forces and moments on the body.
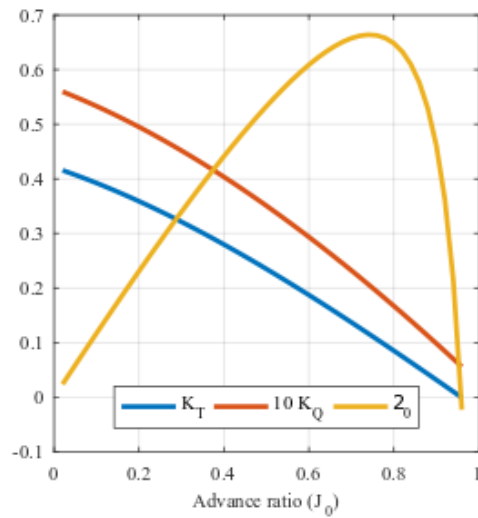
Fig. 14 Open water characteristics

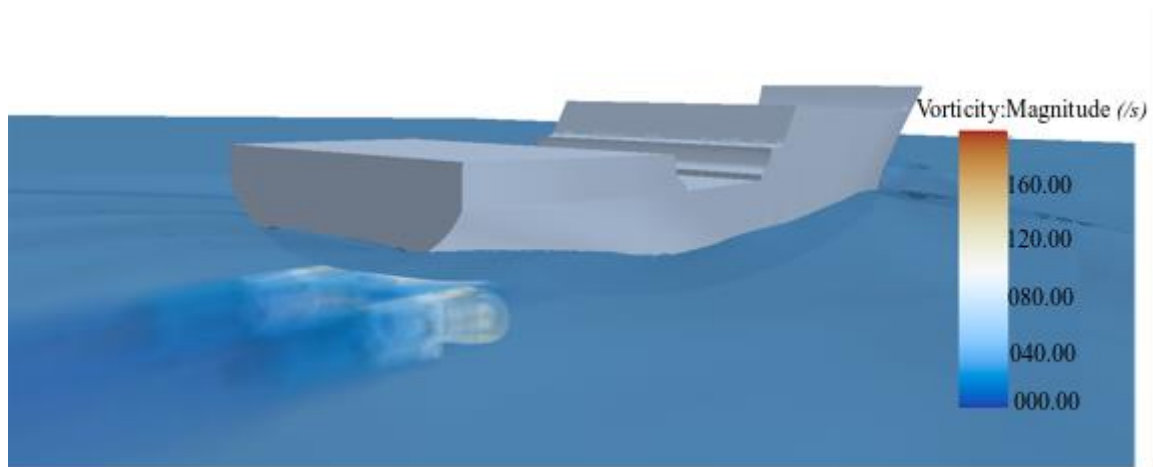Fig. 15 Experimental setup to test open water characteristics of propeller

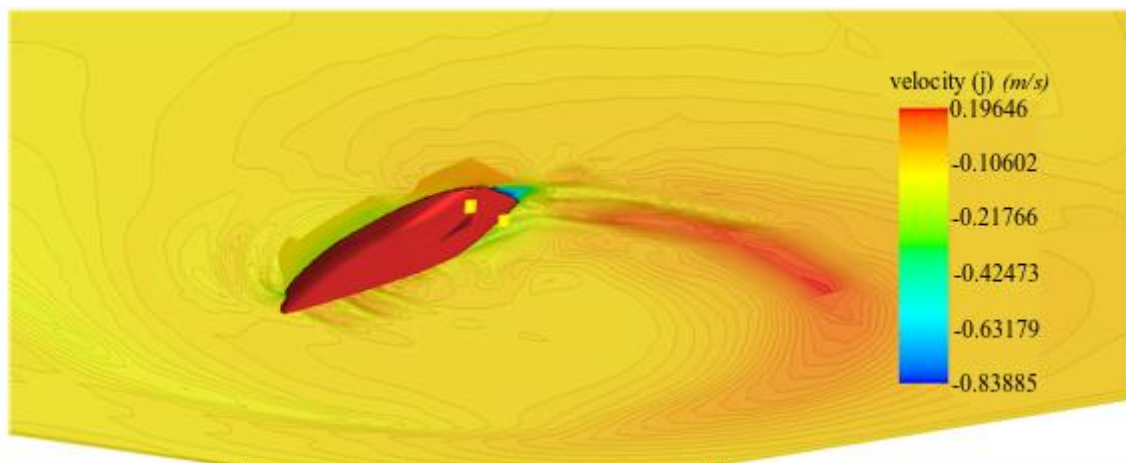Fig. 16 Flow visualisation past the propeller, rudder and hull of ORV during its steady forward movement

Fig. 17 View from the bottom turning manoeuvre of ORV

5.1 Turning circle test

The propeller motion is modelled using virtual disk model of StarCCM+ which is time saving and provides a good prediction of thrust produced by the propeller. Virtual disk model is based on the open water hydrodynamic characteristics of the ORV propeller shown in Fig. 14. The open water characteristics are estimated for a scaled down propeller manufactured in stainless steel using rapid prototyping. The propeller (Wageningen B-Series (B5-75) P/D = 0.903) is fitted to an open water dynamometer setup (Fig. 15). The open water setup consist of a dynamometer to measure thrust and torque, an AC servometer with feedback to provide shaft rotation and submersible streamlined housing to protect the instrument. The setup is fixed to towing tank carriage; and carriage is run at different speed ranging from zero to high value of advance coefficient J. The virtual disk model uses a constant revolution technique to model the propeller from zero to self-propulsion point. Propeller

model is updated at each time step to estimate the thrust and torque from open water data of propeller and applied to the ship model in 6DOF dynamic solver. The spinning motion of water particles by virtual disk behind ship model is shown in Fig. 17. Turning circle test is simulated with a forward speed of 1.5 m/s which is design speed of the vessel. When the model reaches at self-propulsion point rudder is deflected to 35 degree at a constant rate of 0.18 rad/s to make the model turn. The rudder rate is scaled down from 2.5°/s from full scale. Flow visualisation and orientation of ORV vessel during turning circle manoeuvre is shown in Fig. 16. The resulting turning circle parameters are estimated from the turning circle trajectory.
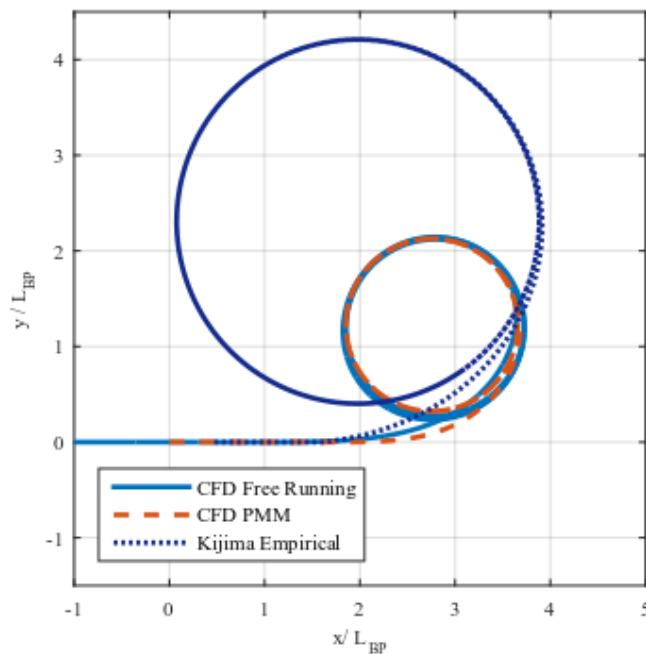
Fig. 18 Trajectory of ship in xy plane

Table 4 Turning circle comparison

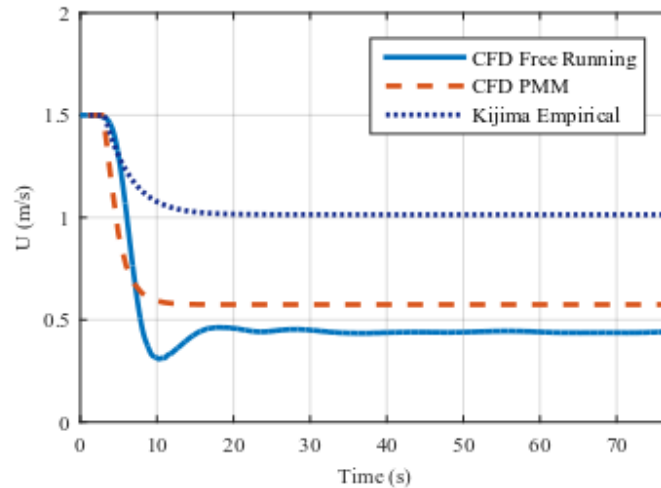|	Free Running	PMM	Empirical
Tactical diameter	2.145 L	2.145 L	4.212 L
Advance	2.730 L	2.680 L	2.912 L
Transfer	1.060 L	0.950 L	2.461 L

Fig. 19 Speed drop during turning circle manoeuvre

6. Results and discussion

Planar Motion Mechanism (PMM) test and free running model tests are numerically simulated in a CFD environment for an Oceanographic Research Vessel (ORV) using RANS based CFD solver, Star CCM+. Estimated hydrodynamic forces and moments from the simulated PMM tests are analysed to obtain hydrodynamic derivatives using Fourier series expansion method. Obtained hydrodynamic derivatives (refer Table 3) are fitted into the manoeuvring mathematical model (refer Eqs. (1) to (10)) to simulate standard manoeuvres. IMO has prescribed standard manoeuvres like turning circle test, zig-zag test and stopping test to identify the manoeuvring characteristics of conventional surface ships. Turning circle trajectory for the model is simulated at a rudder angle of 35° using numerically determined hydrodynamic derivatives are shown in Fig. 18. A comparison of this trajectory is made with the numerically simulated trajectory of free running model tests and trajectory simulated using empirically obtained hydrodynamic derivatives. Speed drop during the turning circle manoeuvre in PMM simulations, Empirically obtained derivative simulations and free running simulations are plotted in Fig. 19. Trajectory obtained from numerically simulated free running model tests match well with the trajectory obtained from the PMM results. Simulation using empirically obtained hydrodynamic derivatives give a larger turning circle trajectory. Estimated turning circle parameters from turning circle simulations are given in Table 4. The parameter obtained from CFD PMM simulation and CFD free running simulation are in good agreement. Empirically obtained derivatives overpredicts these parameters. Tactical diameter is found to be same for both the trajectory obtained from free running model simulations and PMM simulations. Advance shows a deviation of 1:83% form free running simulations to PMM simulations. Transfer shows a deviation of 10:337% from free running simulations to PMM simulations.

7. Conclusions

This paper is an attempt to predict and understand manoeuvring ability of an oceanographic research vessel. Two different numerical methods are adopted. A turning trajectory is simulated by solving equation of motions. The hydrodynamic derivatives required in these equation of motion are found using numerical planar motion mechanism test. In the second approach, a free running turning circle is numerically simulated. Virtual disk approach for propeller is used to save the computation time, where the propeller open water characteristics are obtained experimentally using open water setup in the towing tank facility at IIT Madras. It is found that turning trajectory and speed during turning circle manoeuvre in both cases the model have good match. The advance, transfer and tactical diameter in turning circle manoeuvre obtained using both the approach compare well and are within the IMO requirements. The simulations results are also compared with simulations from empirically obtained hydrodynamic derivatives, it is found that empirically obtained derivatives over-predicts the turning circle trajectory. It can be concluded that modular mathematical model approach, which is computationally more efficient to the numeric free running model test is a reliable one.

References

Abkowitz, M.A. (1964), Lectures on ship hydrodynamics–steering and manoeuvrability.

Alex, G. and Morton, G. (1962), Planar motion mechanism and system. US Patent 3,052,120.

Balagopalan, A., Tiwari, K., Rameesha, T. and Krishnankutty, P. (2019), "Manoeuvring prediction of a container ship using the numerical pmm test and experimental validation using the free running model test", *Ships Offshore Struct.*, 1-14.

Broglia, R., Dubbioso, G., Durante, D. and Di Mascio, A. (2013), "Simulation of turning circle by cfd: Analysisof different propeller models and their effect on manoeuvring prediction", *Appl. Ocean Res.*, **39**, 1-10.

Carrica, P.M., Ismail, F., Hyman, M., Bhushan, S. and Stern, F. (2013), "Turn and zigzag maneuvers of a surface combatant using a urans approach with dynamic overset grids", *J. Mar. Sci. Technol.*, **18**(2), 166-181.

Carrica, P.M., Mofidi, A., Eloot, K. and Delefortrie, G. (2016), "Direct simulation and experimental study ofzigzag maneuver of kcs in shallow water", *Ocean Eng.*, **112**, 117-133.

Cura-Hochbaum, A. (2011), "On the numerical prediction of the ship's manoeuvring behaviour. Cienciay tecnologia de buques", **5**(9), 27-39.

Cura-Hochbaum, A. and Uharek, S. (2016), "Prediction of ship manoeuvrability in waves based on rans simulations", *Proceedings of the 31st Symposium on Naval Hydrodynamics Monterey*, California.

Dash, A.K., Nagarajan, V. and Sha, O.P. (2015), "Uncertainty assessment for ship maneuvering mathematica lmodel", *Int. Shipbuild. Progress*, **62**(1-2), 57-111.

Duman, S. and Bal, S. (2017), "Prediction of the turning and zig-zag maneuvering performance of a surface combatant with urans", *Ocean Syst. Eng.*, **7**(4), 435-460.

Hirano, M., *et al.* (1981), "Hydrodynamic derivatives in ship maneuvering", *Int. Ship Build. Progress*, (325).

Hooft, J., Nienhuis, U., Hutchison, B., Daidola, J., Jakobsen, B. and Ankudinov, V. (1994), "The prediction of the ship's maneuverability in the design stage. discussion. authors' closure", *T. Soc. Naval Archit. Marine Engineers*, **102**, 419-445.

Janardhanan, S. (2010), Numerical estimation of hydrodynamic derivatives in surface ship maneuvering. PhD thesis, IIT Madras.

Jeong, D.H., Roh, M.I. and Ham, S.H. (2017), "Case study of detection and maneuvering performance of naval ships using engagement simulation of engineering level", *Ocean Syst. Eng.*, **7**(3), 247-273.

Karllstrom, C.G. and Astrom, K.J. (1981), "Experiences of system identification applied to ship steering", *Automatica*, **17**(1), 187-198.

Kijima, K. and Nakiri, Y. (1990), Prediction method of ship manoeuvrability in deep and shallow waters.

Kvale, J.M. (2014), Revised simulation model for a very large crude carrier (vlcc). Master's thesis, Norwegian University of Science and Technology, Norway.

Lee, H.Y. and Shin, S.S. (1998), The prediction of ship's manoeuvring performance in initial design stage. In: Proceedings of the PRADS practical design of ships and other floating bodies conference, Maritime Research Institute Netherlands, The Hague, 633-639.

Liu, H. and Ma, N. and Gu, X. (2015a), "Maneuvering prediction of a vlcc model based on cfd simulation for pmm tests by using a circulating water channel", *Proceedings of the 34th International Conference on Ocean, Offshore and Arctic Engineering*, American Society of Mechanical Engineers Digital Collection

Liu, X. and Wan, D. (2015b), "Numerical simulation of ship yaw maneuvering in deep and shallow water", *Proceedings of the 25th International Ocean and Polar Engineering Conference, International Society of Offshore and Polar Engineers.*

Mofidi, A. and Carrica, P.M. (2014), "Simulations of zigzag maneuvers for a container ship with direct movingrudder and propeller", *Comput. Fluids*, **96**, 191-203.

Mofidi, A., Martin, J.E. and Carrica, P.M. (2018), "Propeller/rudder interaction with direct and coupled cfd/potential flow propeller approaches, and application to a zigzag manoeuvre", *Ship Technol. Res.*, **65**(1), 10-31.

Nonaka, K., Miyazaki, H., Nimura, T., Ueno, M., Hino, T. and Kodama, Y. (2000), "Calculation of hydrodynamic forces acting on a ship in maneuvering motion", *Proceedings of the International Conference on Marine Simulation and Ship Maneuvering (MARSIM)*, Orlando, FL, May.

Ohmori, T. (1998), "Finite-volume simulation of flows about a ship in maneuvering motion", *J. Marine Sci. Technol.*, **3**(2), 82-93.

Prasad, B. and Dhanak, M. (2018), "Hydrodynamics of advanced-hull surface vehicles", *Proceedings of the OCEANS 2018MTS/IEEE Charleston*, IEEE.

Rameesha, T. and Krishnankutty, P. (2018), "Numerical study on the manoeuvring of a container ship in regular waves", *Ships Offshore Struct.*, 1-12.

Shen, Z., Wan, D. and Carrica, P.M. (2014), "Rans simulations of free maneuvers with moving rudders and propellers using overset grids in openfoam", *Proceedings of the SIMMAN workshop on Verification and Validation of Ship Maneuvering Simulation Methods*, Lyngby, Denmark.

Shen, Z., Wan, D. and Carrica, P.M. (2015), "Dynamic overset grids in openfoam with application to kcsself-propulsion and maneuvering", *Ocean Eng.*, **108**, 287-306.

Shenoi, R. (2016), Estimation of ship maneuvering hydrodynamic derivatives including roll-effects using ranse based cfd. PhD thesis, Indian Institute of Technology Madras, Chennai, India.

Shenoi, R.R., Krishnankutty, P. and Selvam, R.P. (2016), "Study of maneuverability of container ship withnonlinear and roll-coupled effects by numerical simulations using ranse-based solver", *J. Offshore Mech. Arctic Eng.*, **138**(4), 041801.

Shigunov, V., Guo, B., Reddy, D. and Lalovic, I. (2019), "Manoeuvrability in adverse conditions: Case studies", *Ocean Eng.*, **179**, 371-386.

Skjetne, R., Smogeli, O. and Fossen, T.I. (2004), "Modeling, identification, and adaptive maneuvering of cybership II: A complete design with experiments", *IFAC Proceedings*, **37**(10), 203-208.

Son, K. and Nomoto, K. (1981), "On the coupled motion of steering and rolling of a high speed containership", *J. Soc. Naval Archit. Japan*, **1981**(150), 232-244.

Stern, F., Agdrup, K., Kim, S., Hochbaum, A., Rhee, K., Quadvlieg, F., Perdon, P., Hino, T., Broglia, R. and Gorski, J. (2011), "Experience from simman 2008—the first workshop on verification and validation of ship maneuvering simulation methods", *J. Ship Res.*, **55**(2), 135-147.

Strom-Tejsen, J. (1966), "A model testing technique and method of analysis for the prediction of steering and manoeuvering qualities of surface vessels", Hydro Og Aerodynamisk Laboratorium, Rep Hy 7.

MK

Nomenclature

B	Breadth of the ship (m)
C_B	Block coefficient
C_M	Midship area coefficient
D	Depth of ship
F_N'	Rudder normal force
I_z	Moment of Inertia in Z direction
L_{bp}	Length between perpendiculars (m)
L_{wl}	Length water line (m)
m	Mass of ship (kg)
N_H	Yaw moment acting on ship hull
N_P	Yaw moment due to propeller
N_R	Yaw moment due to rudder
N_r'	Derivative of yaw moment with respect to yaw rate
N_{rrr}'	Third order coupled hydrodynamic derivative of yaw moment with respect to yaw rate
$N_{\dot{r}}'$	Derivative of yaw moment with respect to yaw acceleration
N_v'	Derivative of yaw moment with respect to sway velocity
$N_{\dot{v}}'$	Derivative of yaw moment with respect to sway acceleration
N_{vrr}'	Third order cross coupled hydrodynamic derivative of yaw moment with respect to sway velocity and yaw rate
N_{vvr}'	Third order cross coupled hydrodynamic derivative of yaw moment with respect to sway velocity and yaw rate
N_{vvv}'	Third order coupled hydrodynamic derivative of yaw moment with respect to sway velocity
r	Yaw rate (rad/s)
$\dot{r}$	Yaw acceleration (rad/s^2)
S	Wetted surface area ($m2$)
t'	Non dimensional time
t_p	Thrust deduction factor
T	Draft of the ship (m)
τ_p	Propeller thrust
U_m	Model speed (m/s)
$\dot{u}$	Surge acceleration (m/s^2)
v	Sway velocity (m/s)
$\dot{v}$	Sway acceleration ($m=s2$)
δ	Rudder angle (deg)
$X_{\dot{u}}'$	Hydrodynamic derivative in surge with respect to surge acceleration
x_R	Longitudinal position of rudder (m)

X_H	Surge force acting on ship hull
X_P	Surge force due to propeller
X_R	Surge force due to rudder
X'_{rr}	Second order hydrodynamic derivative of surge force due to sway yaw rate
$X'_{u\|u\|}$	Second order hydrodynamic derivative of surge force due to surge velocity
X'_{vv}	Second order hydrodynamic derivative of surge force due to sway velocity
y_0	Sway amplitude for PMM test
Y_H	Sway force acting on the hull
Y_P	Sway force due to propeller
Y_R	Sway force due to rudder
Y'_r	Hydrodynamic derivative of sway force with respect to yaw rate
Y'_{rrr}	Third order coupled hydrodynamic derivative of sway force with respect to yaw rate
$Y'_{\dot{r}}$	Hydrodynamic derivative of sway force with respect to yaw acceleration
Y'_v	Hydrodynamic derivative of sway force with respect to sway velocity
$Y'_{\dot{v}}$	Hydrodynamic derivative of sway force with respect to sway acceleration
Y'_{vrr}	Third order cross coupled hydrodynamic derivative of sway force with respect to sway velocity and yaw rate
Y'_{vvr}	Third order cross coupled hydrodynamic derivative of sway force with respect to sway velocity and yaw rate
Y'_{vvv}	*Third order coupled hydrodynamic derivative of sway force with respect to sway velocity*
ψ_0	*yaw angle for pure yaw motion*
ω_1	*Frequency of oscillation for pure sway motion*
ω_2	*Frequency of oscillation for pure yaw motion*

Appendix: Hydrodynamic Coefficient Estimation

Fourier series representation for any signal is give as,

$$F(t) = a_0 + \sum_{m-0}^{\infty} a_m \cos m\omega t + b_m \sin m\omega t$$

$$a_0 = \frac{1}{T} \int_0^T f(t)dt$$

$$a_m = \frac{1}{T} \int_0^T f(t) \cos(m\omega t)dt$$

$$b_m = \frac{2}{T} \int_0^T f(t) \sin(m\omega t)dt$$

The force and moment obtained from PMM for different modes can be written as

$$F_{ij} = a_{ij0} + \sum_{m-0}^{3} a_{ijm} \cos m\omega t + b_{ijm} \sin m\omega t$$

Where, $i \in (X,Y,N)$ are the forces and moment recorded during PMM trial. $J \in (PS,PY,MM)$ are the different modes of PMM. Formulae used for calculating hydrodynamic derivatives from Fourier coefficient are as follows

$$v_{a1} = y_0 \omega_1$$

$$v_{a2} = y_0 \omega_2$$

$$u_{on} = \frac{v_{a2}^2}{4u_m}$$

$$u_{cn} = u_m + u_{on}$$

$$u_{cn} = u_m + u_{on}$$

$$v_{0yn} = -u_m \psi_0 - v_{a2}$$

$$u_{0yn} = \frac{v_{a2}\psi_0}{2}$$

$$u_{cyn} = u_m + u_{0yn}$$

$$X_{u|u|} = \frac{a_{110} - a_{112}}{u_m^2}$$

$$X_{vv} = \frac{2a_{112}}{v_{a1}^2}$$

$$Y_{\dot{v}} = \frac{b_{121}}{v_{a1}\omega_1}$$

$$Y_v = \frac{a_{121} - 3a_{123}}{v_{a1}}$$

$$Y_{vvv} = \frac{-4a_{123}}{v_{a1}^3}$$

$$N_{\dot{v}} = \frac{b_{131}}{v_{a1}\omega_1}$$

$$N_v = \frac{-a_{131} - 3a_{133}}{v_{a1}}$$

$$N_{vvv} = \frac{-4a_{133}}{v_{a1}^3}$$

$$X_{\dot{u}} = \frac{-b_{212}}{2u_{0n}\omega_2}$$

$$X_{rr} = -\frac{2(a_{212}u_m^2 - 2a_{110}u_{cn} + 2a112u_{cn}u_{on})}{r_a^2 u_m^2}$$

$$Y_{\dot{r}} = \frac{a_{221}}{r_a\omega_2}$$

$$Y_r = \frac{b_{212}r_a u_{cn} + b_{212}r_a u_{0n} + 2b_{221}u_{0n}\omega_2 + 6b_{223}u_{0n}\omega_2}{2r_a u_{0n}\omega_2}$$

$$Y_{rrr} = \frac{b_{212}r_a + 4b_{223}\omega_2}{r_a^3 \omega_2}$$

$$N_{\dot{r}} = \frac{a_{231}}{r_a\omega_2}$$

$$N_r = \frac{b_{231} + 3b_{233}}{r_a}$$

$$N_{rrr} = \frac{-4b_{233}\omega_2}{r_a^3}$$